CHAPTER 4
AGGLOMERATION OF SUBMICRON PARTICLES BY NTP TECHNIQUE

In this chapter, a technique for the removal of submicron particles with a size range of 0.3-5.0 μm generated in an exhaust gas from diesel oil combustion by a non-thermal plasma (NTP) electrostatic precipitator (ESP) is presented. Plasma agglomeration is presented as a promising process to reduce the concentration of submicron particles in the ESP. An experimental unit consisted of a wire-plate ESP with a saw-tooth electrode. The submicron particle agglomerations were controlled under the operating conditions, such as the supplied pulse peak voltages with nanosecond pulse excitation, the pulse frequencies, the dust loadings, and the mean gas flow velocity. The particle reduction efficiency, which is the concentration of the particles of a certain size reduced at the downstream compared to that at the upstream, was taken as an indicator of the particle removal performance.

4.1 Introduction

Now a day, Air pollutants due to particle emission from combustion exhausts are worldwide investigated. Because, research result shows that particles in the range of micrometer in diameter or smaller that are suspended in air have significant effects on human health, the global climate and the air quality. Specially, submicron particles have been proved to be very harmful to the human organism, children, the elderly and sick people (D. R. Chen *et al.* 1997). Due to submicron size and high superficial area, thus they can be absorb toxic substances and are directly associated with asthma, bronchitis and, loss of breathing capacity, and they have been implicated as a cause for the decrease in life expectancy (K. Donaldson *et al.* 1998). Therefore, there is a need to develop efficient and economical techniques to control these emissions.

ESPs have been widely used to separate particulates from exhaust gas streams. An ESP is characterized by high overall mass collection efficiency (above

90%) with a low-pressure drop and low electrical energy consumption. However, the particulate collection efficiency of the ESP in terms of the number of particles observed is less than 50% (A. Zukeran *et al.* 1999). Most of the submicron particles of 0.1–1.0 μm in diameter can escape from an ESP (M. Mohr *et al*. 1996), and thus it is of great importance to enhance the existing technology for better performance in terms of the submicron particle removal.

One of the most effective and economical methods for improving the collection efficiency of ESPs is particle agglomeration which is a process where the submicron particles are adhered to form a larger one after that can be detected and removed easily. Many techniques of particle agglomeration have been proposed such as: I) the chemicals agglomeration of submicron particles, II) the laminar flow ESPs to promote the surface agglomeration, III) the acoustic agglomeration of dust particles suspended in a gas, IV) the AC or DC electric field agglomeration of charged particles suspended in a gas, and V) the bipolar charging of particles in a gas stream for electrostatic attraction.

E. Riera-Franco de Sarabia *et al.* (E. Riera-Franco de Sarabia *et al.* 2003) used ultrasound to enhance the agglomeration of particles in a range of diameters of a micrometer or smaller. However, this technique was rather expensive to be implemented in a large scale. Mitchner and Self (M. Mitchner and Self 1983), Kobashi (M. Kobashi 1978), Kildeso *et al.* (J. Kildeso *et al.* 1995) , and Laitinen *et al.* (A. Laitinen *et al.* 1996**)** studied the effect of bipolar charging on the small particle agglomeration efficiency of a parallel plate agglomerator. Mitchner and Self conducted a series of experiments to measure the different charge-to-mass ratios of particles by corona charging and reported that the charging process became less effective at higher particle concentration. Watanabe *et al.* (T. Watanabe *et al.* 1995) performed experiments with a quadrupole field, where particles were charged and agglomerated by an AC voltage superimposed with a DC voltage. Hautanen *et al.* (J. Hautanen *et al.* 1995) experimentally investigated the AC agglomeration of unipolar charged particles with both parallel plate and quadrupole agglomerators. Eliasson and Egli (B. Eliasson and W. Egli 1991) proposed an agglomerator based on bipolar particle charging to increase the rate of particle coagulation. Masuda utilized pulsed corona plasma to remove NO_X and SO_2 in flue gas, which was promoted as a

technology for many applications in the area of pollution control (S. Masuda and H. Nakao 1986). The high capture efficiency of $PM_{2.5}$ particles from a coal-fired power plant by pulsed corona discharge combined with DC agglomeration was also reported (F. Xu *et al.* 2008).

NTP can be generated by applying high-voltage pulses to electrodes with small diameters or sharp edges in the ESP. The required voltage depends on the distance between the electrodes, and the pulse duration. The pulse duration is normally less than 1 μs, and its rise time is approximately ten nanoseconds. This voltage pulse can lead to a significant electric field stress during the duration of the pulse without causing spark breakdown as in the normal ESP. As a result, energetic electrons can be generated without raising the ion temperature (Wook Hee KOH and In Ho PARK 2003), and the submicron particles can be charged with different polarities. An attractive force between differently charged particles can be created, and the agglomeration of submicron particles in a plasma field from tens of nanometers can be increased to millimeter- sized particles that can be easily collected.

However, the submicron particle agglomerations by pulsed corona plasma have not yet been discussed in more details. In this paper, a wire-plate ESP with an energized pulse corona was designed and operated under controlled operating conditions using different pulse peak voltages (V_p), pulse frequencies (f), dust loadings (N) and gas flow velocities (U_g).

4.2 Theory

4.2.1 Positive Pulse Corona Charging of Submicron Particles

Under NTP, which is generated from positive pulse corona discharges, a large number of negatively charged particles appeared. The number ratio of negatively charged particles to positively charged ones increased as the peak value of pulse voltage increased. The process of particle charging by positive pulse corona discharges can be divided into four stages follow as:

(a) Streamer propagation stage: The streamer on-set voltage is higher than the corona on-set voltage and increases with increasing velocity of pulsed voltage in duration time of about 30 ns. The initial electron avalanche propagates rapidly with light ionization and produces streamer discharges from the positive

electrode to the negative electrode. When stop the pulsed voltage suddenly the streamer propagation is also terminated immediately. In this stage, the electrons move to the positive electrode along the leads of streamer discharges. Both positive and negative ions cannot move in such a short time. Only the electrons charge the particles in the vicinity between electrodes and the charging mechanism on the particles is governed by the free electron. Therefore, the particles are negatively charged in this stage.

(b) Migration and diffusion stage of free electrons: This stage continues for approximately 150 ns. After the streamer propagation stage finished, the electrons move along the electric lines of force and diffuse to the low-concentration region of electrons. Ions still remain motionless in this short stage and only free electrons can charge the particles. This process is understandable, because the free electron diffusivity-mobility ratio is so high that the electrons can charge the particles beyond the ion field-charging limit. The particles are further negatively charged by the electrons, which is similar to the diffusion charging by ions.

(c) Positive corona discharge stage: This stage is during about 200 μs, which is much longer than the above two stages. The start point of this stage corresponds to the corona on-set voltage, which is determined by the Peek formula. The end of this stage corresponds to the moment, at which both the migration and the diffusion of free electrons stop. At the starting point of this stage, some free electrons produced by the streamer discharges have completely moved into the positive electrode and the others have attached onto electronegative gas molecules to form negative ions. After that, the streamer discharges change into corona discharges, according to the gentle down slope of the voltage waveform. Except for the positive and negative ions produced by pulsed streamer discharges in the above two stages, the corona discharges generate continual positive ions. Both the positive and the negative ions start moving in opposite directions and recombine with each other along the way. In the charging process, negative charges of the particles charged in the above two stages are gradually decreasing by means of the field-diffusion charging of dipolar ions. Some particles start the positive charging process, because there are more positive ions than negative ions between the electrodes.

(d) Ion migration stage: This stage is about 100 μs. The start point of this stage corresponds to the moment, at which the whole charging process stops. When the pulsed voltage drops below the corona onset voltage after the positive corona discharge stage finished, the corona discharges stop. In the electrode space, new ions are not present. The residual bipolar ions continually move in opposite directions and recombine with each other along the way. During this stage, positive ions play a dominant role in the charging process of bipolar ions. As the electric field decreases and the charging process of positive ions develop, positive charge depletion zones are formed and gradually increase around the positively charged particles. Therefore, more and more positive ions cannot reach the positively charged particles because of the field charging mechanism of ions, and the diffusion charging rate of positive ions on positively charged particles is gradually lowered. Finally, some particles still remain with negative charges and others are neutralized or consequently charged with positive charges. Therefore, both positively and negatively charged particles occur under positive pulse corona discharges.

When the peak value increases in the range of the pulsed streamer corona discharges, the charging effects of electrons obviously increase in stages (a) and (b). Although the concentrations of the dipolar ions are increased, the positive ions produced by positive corona discharges have no change in stage (c). Positively charging effects show little increase in stages (c) and (d). Therefore, the number of negatively charged particles can obviously exceed the number of positively charged ones, when the peak value of pulse corona voltages is sufficiently high.

4.2.2 Plasma agglomeration

When the distance between the dust particles with opposite charges becomes less than a critical length, λ_D, they make coagulation and the change of the coagulating grains, and the radius becomes large. For non-thermal equilibrium condition, $\lambda_D$could be evaluated by

$$\lambda_D = \sqrt{\frac{kT_e}{4\pi e^2 N_e}}. \tag{4.1}$$

Where e is electron charge, k is Boltzmann's constant, N_e is electron density, and T_e is electron temperature.

The electron energy in function of the applied electric field is empirically given by the following equation:

$$kT_e = a + b\frac{E}{N} + c\left(\frac{E}{N}\right)^2 . \tag{4.2}$$

Where a, b and c are empirical coefficients, $\frac{E}{N}$ is reduced field strength in unit Townsend (Td). The energy injected in to corona discharge can be divided in to two parts; the first part is called active energy injection for streamer head propagation and the second one is passive energy injection after streamer stops.

The model used to estimate the number of elementary charge $Z_p$carried by particle is

$$n_p = \frac{4\pi\varepsilon_0}{e} r_p V_s. \tag{4.3}$$

Where V_s particle potential estimated by equalizing the electron and the ion currents leads to

$$1 - \tau\,\Delta = \frac{N_e}{N_i}\sqrt{\frac{m_i}{m_e}}\,\tau\exp(\Delta). \tag{4.4}$$

Where $\tau = \frac{T_e}{T_i}$, and $\Delta = \frac{eV_s}{kT_e}$

The electrostatic potential field given by each particle at the distance of r is calculated from

$$V(r) = \frac{n_p e}{4\pi\varepsilon_0 r} exp\left(\frac{r}{\lambda_D}\right). \tag{4.5}$$

If $r_p \ll \lambda_D$ then the potential energy between particles in plasma in spherical coordinates is given by

$$qV = \frac{n_p^2 e^2}{4\pi\varepsilon_0(r_{p1}+r_{p2})}. \tag{4.6}$$

When the distance between the dust particle is $(r_{p1} + r_{p2)}$ with electric charge, $z_p e$.

In estimating the binding energy of particle agglomerates a simple model is deployed by assuming that the radius r_p of sphere particle is significantly less than the Debye lengthλ_D. The energy balance on the particle agglomeration is given by

$$\frac{n_p^2 e^2}{4\pi\varepsilon_0(r_{p1}+r_{p2})} = kT_p. \tag{4.7}$$

By normalizing the energy equation to the thermal energy U_T of particle, we can obtain

$$H = \frac{qV}{kT_p} = \frac{n_d^2 e^2}{4\pi kT_p(r_{p1}+r_{p2})}. \tag{4.8}$$

Under steady state, the rate of the number of particle with radius r_{p2} spreading to the particle with radius r_{p1}will be (T. Minkang and L. Siwen 2006)

$$\frac{dN_{12}}{dt} = \frac{4\pi Dn(r_{p1}+r_{p2})}{\frac{1}{H}[e^H-1]}. \tag{4.9}$$

If $H < 1$, the agglomeration rate of particle will increase under this situation.

If $H > 1$, the agglomeration rate of particle will decrease under this situation because of repulsion.

If $H = 1$, it is the situation that impacted particle have no charges.

The main mechanism of the agglomeration of particle is the result of the particles with opposite polarity charges attracts each other by Coulomb force. Because there is the strong attraction among particles with opposite polarity charges, the probability of particles colliding is increased sharply which induces the particles to be close to each other, which highly induces the agglomeration of particles. Meanwhile, the polarized charge plays a positive role to the agglomeration of particle too.

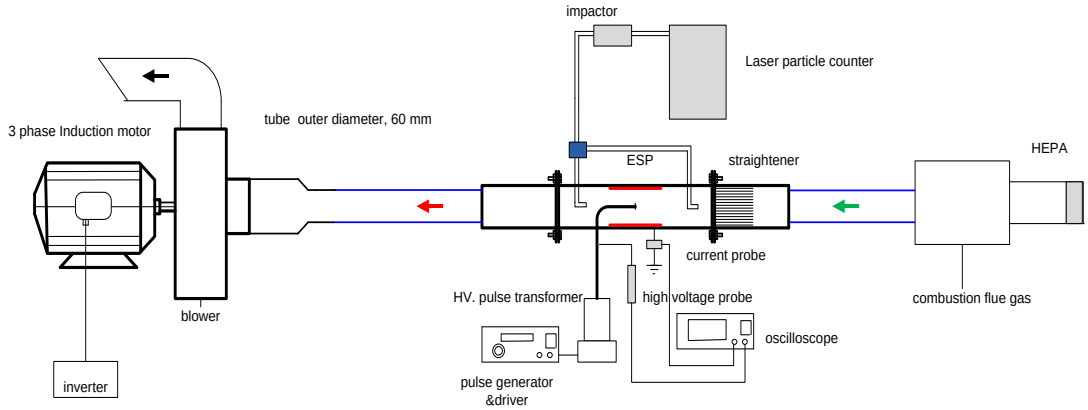

Figure 4.1 The experimental setup.

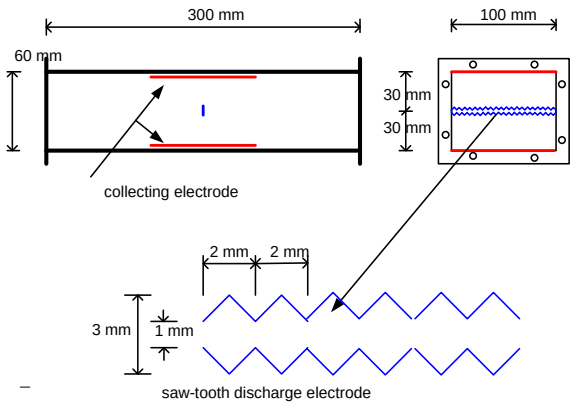

Figure 4.2 The configuration of the ESP electrodes.

4.3. Experimental setup

The experimental setup is shown in Figure 4.1.The system mainly consisted of an exhaust gas supply, ESP electrodes and a high voltage pulse power supply for generating the NTP. The test section was an acrylic duct of 300 mm in length and 100 mm x 60 mm in cross-section. The electrical electrode set consisted of two ground plate electrodes and a saw-tooth discharge electrode. The saw-tooth electrode (100 mm in length) and the plate electrodes (100 mm in width and 200 mm in length) were composed of stainless steel. The saw-tooth electrode was placed midway between the ground plate electrodes. Perpendicular to the gas flow direction, as shown in Figure 4.2, the distance between the saw-tooth and the ground plate electrodes was 30 mm. A gas flow straightener was placed before the reactor inlet. An exhaust gas of diesel combustion from a Bunsen burner was introduced to the test unit at room temperature. The inlet concentration of the carbon particles was adjusted to approximately 5×10^5 particle cm^{-3}, and the gas velocity was controlled by a downstream blower with a speed controller. The typical parameters of the ESP are summarized in Table 4.1. A high efficiency particle filter (HEPA) was installed at the inlet of the duct to obtain aerosol-free inlet air.

A high voltage pulse power supply with a function generator was used in this experiment. The waveform of the voltage was measured by an oscilloscope (Tektronix TDS 2014) and a high voltage probe (Tektronix P644A). The flue gas was sampled and the number of particles related to the particle sizes were classified with a laser particle counter at the upstream and at the downstream of the test section.

Agglomeration is a mass-conserving, but number-reducing process that shifts the particle distribution towards larger sizes. Thus, the agglomeration efficiency can be represented by the reduction efficiency of submicron particles in the NTP ESP. The basic expression of the reduction efficiency for a given particle size range, is the ratio of the number of particles reduced by the agglomeration to the number of particles fed upstream of the test device.

Table 4.1 Basic parameters of the ESP

Parameter	Typical values(normal ESP)	This study(NTP generator)
Gas velocity	1-2 ms^{-1}	0.5-1.5 ms^{-1}
Temperature	100-250 ℃	Room temperature
Electrode Spacing	250-500 mm	30 mm
Electric field	7 kV cm^{-1}	8 kV cm^{-1}
Polarity	negative	positive
Frequency	DC	10-20 kHz

The particle reduction efficiency, $\eta_r(d_p)$ was evaluated with the number concentration of the particles in a certain size fraction measured at the inlet and outlet of the reactor as

$$\eta_r(d_p) = 1 - \frac{N_{out}(d_p)}{N_{in}(d_p)} \ , \tag{4.10}$$

N_{in} is particle number concentration at the test unit upstream (particles cm^{-3}), and N_{out} is the corresponding particle number concentration at the test unit downstream (particles cm^{-3}).

4.4. Results and discussion

4.4.1. Voltage-current characteristics

The plasma generator was supplied by a positive pulsed power to generate different pulse peak voltages and pulse frequencies to generate plasma ionization. The minimum rise time of the generated pulse was approximately 250 ns and the maximum peak voltage was approximately 45 kV_p. The pulse frequency ranged from 10 kHz to 20 kHz. Figure 4.3 shows V-I characteristics of our NTP generator compared with the conventional DC ESP. In the case of positive DC excitation, a corona started at +5 kV. The discharge current sharply increased as the applied voltage exceeded the corona onset voltage and reached approximately 45 μA at +7 kV. When the voltage was increased further, an electrical breakdown occurred, as shown in Figure 4.4(a). For the NTP, a corona started at +12 kV, and the discharge

current increased sharply with the increase of voltage supply due to the short duration of the supplied voltage pulse. The supplied voltage exceeded the corona onset voltage and the peak current reached approximately 500 µA at +17 kV without electrical breakdown as shown in Figure 4.4(b). According to the figure, when the pulse voltage was over the ionization threshold of approximately + 15 kV_p, the plasma streamers could be generated.

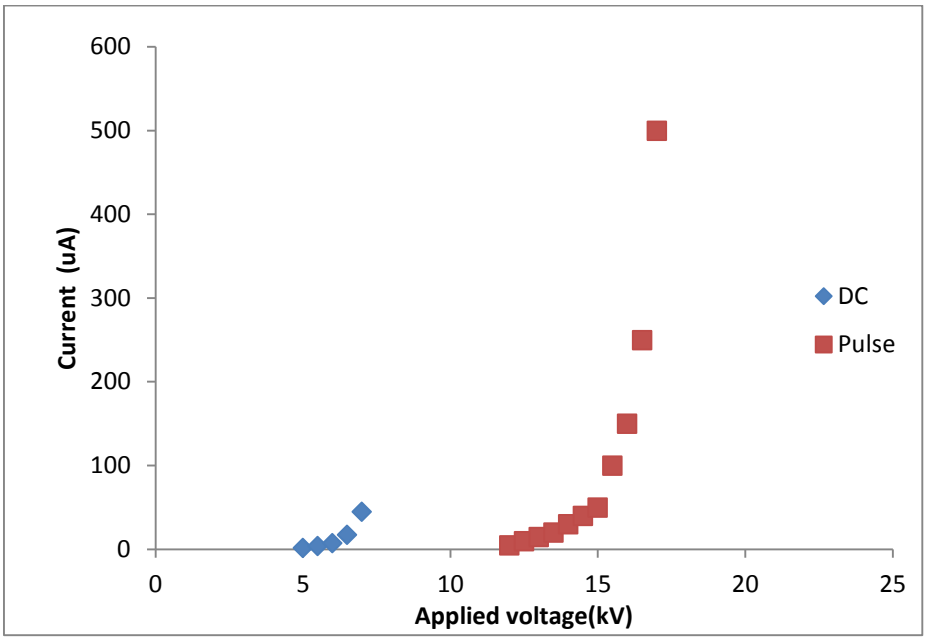

Figure 4.3 Voltage-current characteristics of the ESP generators.

In the plasma generator, non-thermal electrons could be generated through the formation of plasma filaments in the electric field. Then, the plasma streamer could yield a good power efficiency, which consumes a very small energy input.

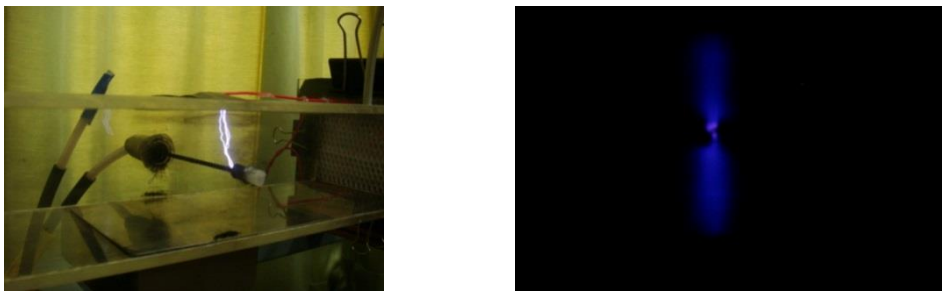

(a) An electrical breakdown. (b) A plasma streamer.

Figure 4.4 (a) An electrical breakdown in a conventional DC ESP and (b) a plasma streamer in our pulse-excited ESP.

4.4.2. Distributions of the particle number concentration

A laser particle counter (LPC) was deployed to measure the distribution of the submicron particle number concentration. The particle number distributions and their accumulative distributions are shown in Figure 4.5. The measured sizes ranged from 0.3 μm to 5 μm. In our experiments, over 100 experimental runs were carried out of which 3 different concentration ranges of particle concentrations could be classified as 1×10^{4}-1.5×10^{4} particles cm^{-3}(low loading), 1.6×10^{5}-2×10^{5} particles cm^{-3} (medium loading) and 4×10^{5}-5×10^{5} particles cm^{-3}(high loading). The results shown in the following Figures are the average values with 95 % confidence interval.

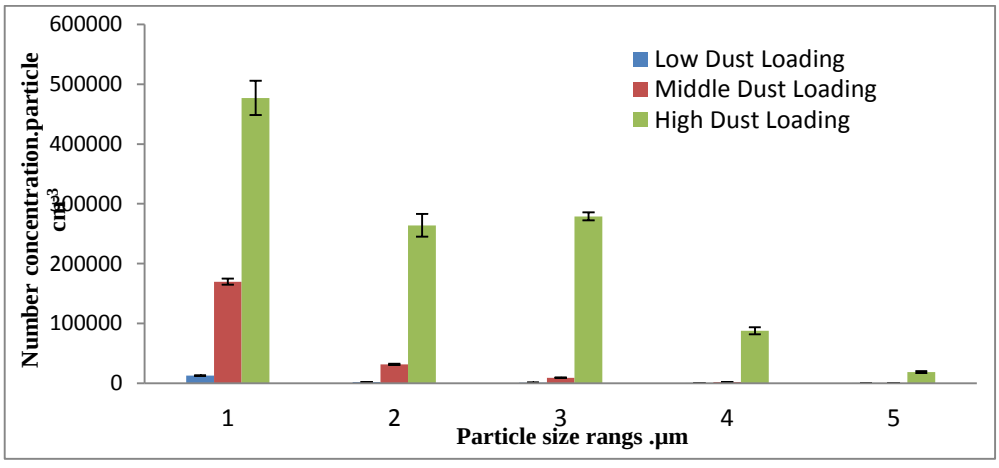

Figure 4.5 Particle size distributions from the LPC (at the inlet).

4.4.3. Agglomeration of submicron particles in NTP ESP

Before testing of particle charging, there were some experimental tests to verify the deposit of particles in the test section. Experimental studies were carried out by feeding the combustion gas having various sizes of submicron into the test section without generated electric field and the numbers of particles at the upstream and the downstream were monitored. Figure 4.6 shows the results and it could be seen that the values at both positions for all distributions of particle sizes were almost similar which meant that very small amount of deposited particles was found.

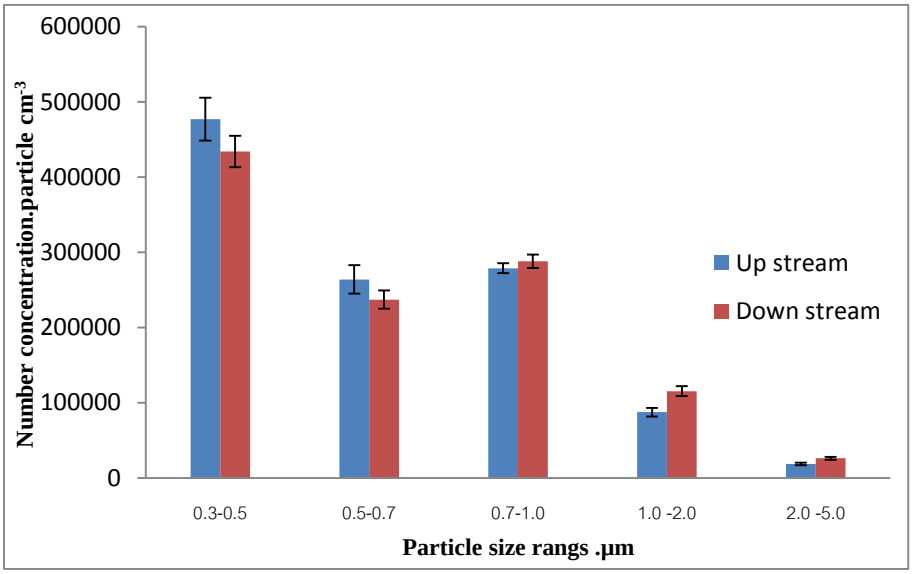

Figure 4.6 Distributions of number of particles entering and leaving the agglomerator when there is no electric field generation.at gas velocity 0.5 m/s and gas temperature 35 ℃.

When the submicron particles were introduced to the NTP ESP, at the upstream of the test section, the particles were very small and could not be observed by eye. When they passed through the plasma field where the agglomeration occurred, the particle sizes were increased and easily detected. The results are shown in Figure 4.6. Some particles fell down due to gravity, as shown in Figure 4.8.

Figure 4.7 The submicron particle agglomeration in the test section.

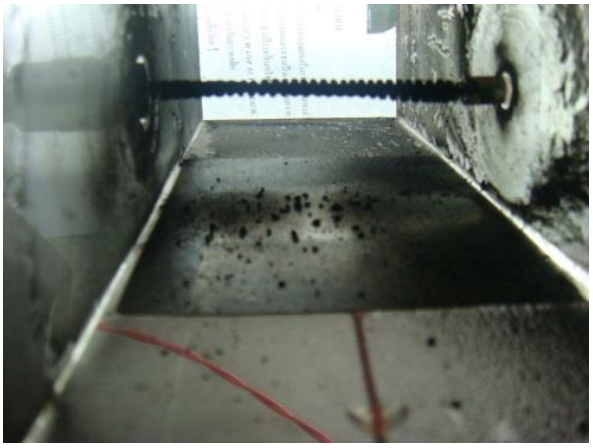

Figure 4.8 The large particles that fell due to the agglomeration.

4.4.4. Effect of the pulse peak voltage on the agglomeration and the particle reduction efficiency

Experiments were conducted to investigate the effects of the pulse peak voltage on the agglomeration of the dust particles in terms of particle reduction efficiency. In Table 4.2, the gas flow velocity was controlled at approximately 1 ms^{-1} to provide a residence time of approximately 0.2 s in the NTP ESP. Experiments were performed by changing the pulse peak voltage with a dust loading and a pulse frequency of 5×10^5 particles cm^{-3} and 20 kHz, respectively.

The number of particles in the ranges of 0.3 – 0.5, 0.5 - 0.7, 0.7 – 1.0, 1.0 -2.0 and 2.0 – 5.0 μm, as given in Figure 4.5, could be reduced with increased peak voltage. Then, the reduction efficiency calculated by equation (4.10) increased. A higher efficiency, especially for the small particles, meant that a better agglomeration of the particles could be achieved, and then the number of small particles remaining decreased.

Table 4.2 The particle reduction efficiencies with various pulse voltages. The dust loading and the pulse frequency were 5×10^5 particles $cm^{-3}$and 20 kHz, respectively. The gas velocity was 1 ms^{-1}.

Voltage, kV	particle size range				
	0.3-0.5 μm	0.5-0.7 μm	0.7-1.0 μm	1.0-2.0 μm	2.0-5.0 μm
15	80.6%	81.9%	96.4%	97.8%	98.1%
25	83.6%	88.9%	96.4%	97.8%	98.7%
35	86.1%	92.1%	97.5%	98.4%	98.12%
45	90.01%	94.94%	98.56%	98.12%	98.5%

4.4.5. Effect of the pulse frequency on the particle reduction efficiency

Experiments were conducted to investigate the effects of the pulse frequency on the particle reduction efficiency. Experiments were performed by setting the particle concentration at approximately 5×10^5 particles cm^{-3} while the pulse peak voltage was constant at 45 kV. The gas flow velocity was controlled to approximately 1 ms^{-1} in the pulse plasma reactor. The particles were more energized with a higher pulse frequency, and thus better agglomeration of the small particles to a greater size could be obtained. As shown in Table 4.3, the higher the pulse frequency was, the higher the particle reduction efficiency.

Table 4.3 The particle reduction efficiency with various pulse frequencies. The particle concentration was at approximately 5×10^5 particles cm^{-3}, and the pulse peak voltage was 45 kV. The gas velocity was 1 ms^{-1}.

Pulse Frequency, kHz	particle size range				
	0.3-0.5 μm	0.5-0.7 μm	0.7-1.0 μm	1.0-2.0 μm	2.0-5.0 μm
13	80.4%	82.5%	86.4%	88.8%	90.7%
15	84.1%	90.9%	93.4%	95.5%	97.3%
20	90.01%	94.94%	98.56%	98.12%	98.5%

4.4.6. Effect of the particle concentration on the particle reduction efficiency

The effect of the dust loading on the particle reduction efficiency was also investigated. Experiments were performed by setting the supplied pulse peak voltage and the pulse frequency to 45 kV and 20 Hz, respectively. The gas flow velocity was controlled at approximately 1 ms^{-1} in the test section. A higher particle concentration led to high rate of particle collision, and thus the small particles could be easily agglomerated. According to Table 4.4, the particle reduction efficiency also increased with the increase of the dust loading.

Table 4.4 The particle reduction efficiency with various dust loadings. The supplied pulse peak voltage and the pulse frequency were 45 kV and 20 Hz, respectively. The gas flow velocity was controlled at approximately 1 ms^{-1}.

particle concentration	particle size range				
	0.3-0.5 µm	0.5-0.7 µm	0.7-1.0 µm	1.0-2.0 µm	2.0-5.0 µm
Low	70.4%	74.5%	78.4%	82.8%	85.7%
Middle	82.1%	85.9%	87.4%	92.5%	94.3%
High	90.01%	94.94%	98.56%	98.12%	98.5%

4.4.7. Effects of the gas flow velocity on the particle reduction efficiency

The effect of the gas flow velocity on the particle reduction efficiency was also investigated. Experiments were performed by setting the supplied pulse peak voltage and the pulse frequency to 45 kV and 20 Hz, respectively. The dust loading was controlled at approximately 5×10^5 particles cm^{-3} . The gas flow velocity was adjusted from 0.5 ms^{-1} to 1.5 ms^{-1} to provide a gas residence time of 0.4 s to 0.133 s in the test section. With a higher gas velocity, a higher frequency of small particle collisions was obtained and the agglomeration of charged small particles could be achieved easily. However, the residence time of electrical charging was lower, and some particles were insufficiently charged. Thus, although there were some collisions, the particles did not adhere to each other.

In Table 4.5, for a gas velocity of 0.5 – 1 ms^{-1}, the charging period was adequate and when the gas velocity increased, the particle reduction efficiency also increased. However, when the velocity was over 1 ms^{-1}, the efficiency tended to decrease because the particle charging period was shortened and the agglomeration process depended mainly on the collision of submicron particles. For our equipment, a residence time of 0.2 s was the optimum for particle agglomeration.

Table 4.5 The particle reduction efficiency with various gas flow velocities. The supplied pulse peak voltage and the pulse frequency were 45 kV and 20 kHz, respectively. The dust loading was controlled at approximately 5×10^5 particles cm^{-3}.

Gas flow velocity, ms^{-1}	particle size range				
	0.3-0.5 µm	0.5-0.7 µm	0.7-1.0 µm	1.0-2.0 µm	2.0-5.0 µm
0.5	80.6%	88.9%	92.4%	95.8%	96.7%
0.8	86.1%	92.1%	97.5%	98.4%	98.12%
1.0	90.01%	94.94%	98.56%	98.12%	98.5%
1.2	88.1%	93.73%	96.38%	95.86%	95.12%
1.5	84.20%	93.39%	95.5%	96.4%	95.12%

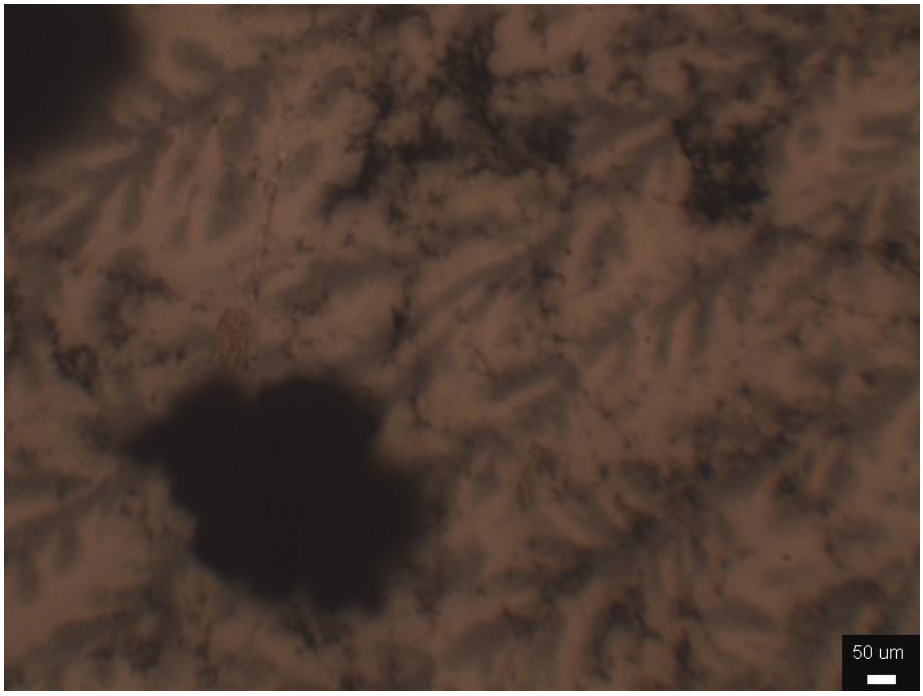

(a) 1.5 ms^{-1} **(100x)**

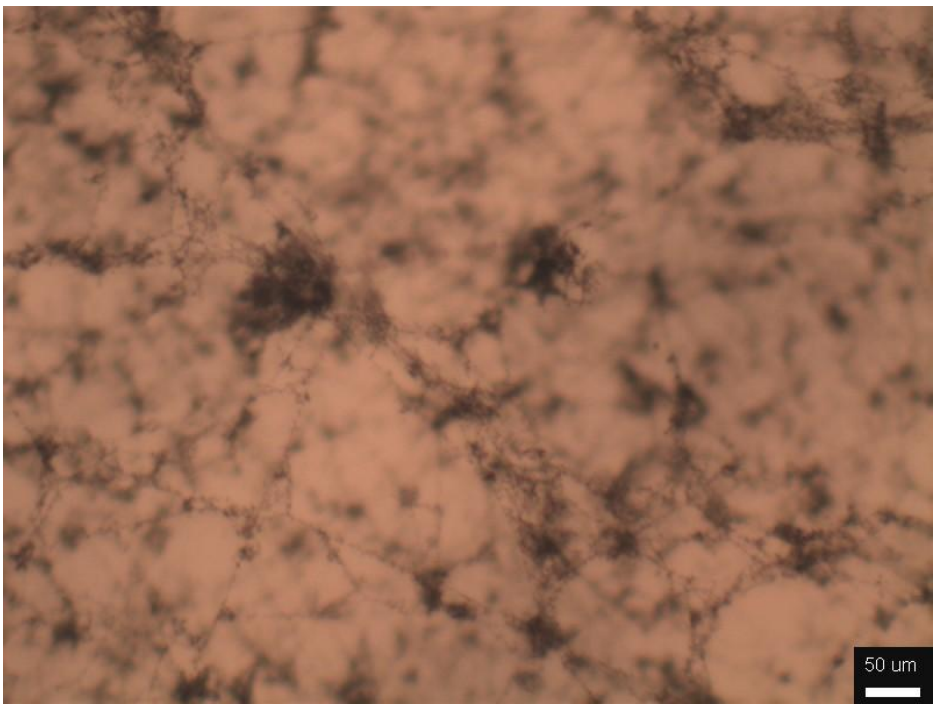

(b) 0.5 ms^{-1}(100x)

Figure 4.9 Agglomerations of submicron particles at different gas velocities.

Figure 4.9 (a) showed samples of submicron particles agglomerated at different gas velocities. The sample at a higher gas velocity was more compact, and the body was more rigid because the agglomeration was mainly due to the collisions while that of the other one as shown in Figure 4.9 (b) was due to the electrostatic force then the structure of the agglomerated particles was more fractal.

4.4.8. Modeling of Agglomeration

The particle reduction efficiency, η_r, was evaluated with the number concentration of the particles in a certain size fraction measured at the inlet and outlet of the reactor under controlled operating conditions using different pulse peak voltages (V_p), pulse frequencies (f), dust loadings (N) and gas flow velocities (U_g) particle size (d_p). Then

$$\eta_r = f(V_p\ , f, N, U_{\mathrm{g}}\ , d_p).\qquad (4.10)$$

The terms, V_{p} and f could be transformed into the average voltage, V_{ave}, as $V_{ave} = V_p \times\ T_d \times\ f$ then the above relation could be rewritten as

$$\eta_r = f(V_{ave}\ , N, U\mathrm{g}\ , d_p).\qquad (4.11)$$

A correlation could be set in a form of

$$\eta_r\ = aV_{ave}^{b1} \times\ N^{b2} \times U_g^{b3} \times {d_p}^{b3}).\qquad (4.12)$$

From our experimental data, the correlation could be

$$\eta_r\ = 91.811 \times V_{ave}^{0.039988} \times\ N^{-0.004392} \times U_g^{0.002238} \times {d_p}^{0.0053816}),\qquad (4.13)$$

15 kV < V_p< 45 kV,

$1\times 10^4\ \frac{particle}{cm^3}$<$N$ <$5\times 10^5\ \frac{particle}{cm^3}$,

0.5 m/s < U_g<2 m/s,

0.3 μm < d_p< 5 μm.

The results from the correlation could fit all the experimental data within 10 % deviation.

4.5 Conclusions

In this paper, a laboratory-scale wire-plate ESP with pulsed corona energization to generate a NTP field is proposed. Experimental studies were performed to investigate the agglomeration characteristics and the reduction efficiency of submicron particles in a size range of 0.3 – 5.0 μm, which were emitted from diesel oil combustion. The controlled conditions were the supplied pulse peak voltages with nanosecond pulse energization, the pulse frequencies, the dust loadings, and the mean gas flow velocity. The particle reduction

efficiency of the number of particles at a certain size was used as an indicator of the particle removal performance.

The experimental results showed that the particle reduction efficiency increased with increasing pulse peak voltage and pulse frequency. The gas velocity also affected the efficiency. With a higher gas velocity, a higher frequency of small particle collisions could be obtained, and the agglomeration of charged small particles could be achieved easily. However, the residence time of electrical charging was lower, and some particles were insufficiently charged. Although there were some collisions, the particles did not adhere to each other. In our experiment at a peak voltage of 45 kV and a pulse frequency at 20 kHz, the efficiency increased when the gas velocity was increased from 0.5 ms^{-1} to 1 ms^{-1}, but a lower efficiency was obtained when the speed was over 1 m/s. In this condition, the submicron particle number reduction efficiency for all particle sizes was over 90% in our NTP ESP.
A model to predict the efficiency at various operating conditions could be evaluated from the experimental data as

$$\eta_r = 91.811 \times V_{ave}^{0.039988} \times N^{-0.004392} \times U_g^{0.002238} \times {d_p}^{0.0053816}),(4.13)$$

15 kV < V_p< 45 kV,

$1\times 10^4 \frac{particle}{cm^3}$<$N$ <$5\times 10^5 \frac{particle}{cm^3}$,

0.5 m/s < U_g<2 m/s,

0.3 μm < d_p< 5 μm.

The results from the correlation could fit all the experimental data within 10 % deviation.